Supporting information for article:

Hydrogen-bond directionality and symmetry in [C(O)NH](N)2P(O)-based structures: a comparison between X-ray crystallography data and neutron-normalized values, and evaluation of reliability

Maryam Taherzadeh, Mehrdad Pourayoubi, Banafsheh Vahdani Alviri, Samad Shoghpour Bayraq, Maral Ariani, Marek Nečas, Michal Dušek, Václav Eigner, Hadi Amiri Rudbari, Giuseppe Bruno, Teresa Mancilla Percino, Marco A. Leyva Ramírez and Krishnan Damodaran

Experimental

1: M.p. 176 °C. Anal. Calc. for $C_{35}H_{33}ClN_3O_2P$ (%): C = 70.76; H = 5.60; N = 7.07; found: C = 70.63; H = 5.83; N = 6.58. $^{31}P\{^1H\}$ NMR (DMSO-d_6): δ = 15.71 (s). ^1H NMR (DMSO-d_6): δ = 4.06 (dd, ^2J(H,H) = 15.3 Hz, ^3J(P,H) = 10.6 Hz, 4H, CH$_{Bz}$), 4.27 (dd, ^2J(H,H) = 15.3 Hz, ^3J(P,H) = 10.2 Hz, 4H, CH$_{Bz}$), 7.18 – 7.86 (m, 24H), 9.91 (br. s, 1H, NH). $^{13}C\{^1H\}$ NMR (DMSO-d_6): δ = 48.53, 127.10, 128.19, 128.38, 130.23, 132.62 (d, ^3J(P,C) = 7.5 Hz), 136.96 (d, ^3J(P,C) = 3.4 Hz), 137.08, 167.76. MS (70 eV, EI): m/z (%) = 595 (< 1) [M + 2]$^+$, 593 (< 1) [M]$^+$, 139 (27) [4-^{35}Cl-C$_6$H$_4$CO]$^+$, 137 (71) [4-^{35}Cl-C$_6$H$_4$CN]$^+$, 106 (74) [C$_7$H$_8$N]$^+$, 91 (100) [C$_7$H$_7$]$^+$. MS (20 eV, EI): m/z (%) = 595 (6) [M + 2]$^+$, 456 (< 1) [P(O)(OH)[N(CH$_2$C$_6$H$_5$)$_2$]$_2$]$^+$, 139 (10) [4-^{35}Cl-C$_6$H$_4$CO]$^+$, 137 (24) [4-^{35}Cl-C$_6$H$_4$CN]$^+$, 106 (79) [C$_7$H$_8$N]$^+$, 91 (100) [C$_7$H$_7$]$^+$.

2: M.p. 187 °C. Anal. Calc. for $C_{21}H_{21}ClN_3O_2P$ (%): C = 60.95; H = 5.11; N = 10.15; found: C = 60.88; H = 5.01; N = 10.07. $^{31}P\{^1H\}$ NMR (DMSO-d_6): δ = 8.90 (s). ^1H NMR (DMSO-d_6): δ = 4.05 (m, 4H, CH$_{Bz}$), 5.04 (m, 2H, NH), 7.14 – 7.90 (m, 14H), 9.40 (br. s, 1H, NH). $^{13}C\{^1H\}$ NMR (DMSO-d_6): δ = 43.71 (d, ^2J(P,C) = 8.2 Hz), 126.48, 127.22, 128.00, 128.31, 129.94, 132.61 (d, ^3J(P,C) = 8.2 Hz), 141.10 (d, ^3J(P,C) = 5.6 Hz), 167.12. MS (70 eV, EI): m/z (%) = 415 (13) [M + 2]$^+$, 413 (20) [M]$^+$, 412 (26) [M − 1]$^+$, 154 (100) [4-^{35}Cl-C$_6$H$_4$C(O)NH]$^+$, 139 (58) [4-^{35}Cl-C$_6$H$_4$CO]$^+$, 137 (48) [4-^{35}Cl-C$_6$H$_4$CN]$^+$, 106 (64) [C$_7$H$_8$N]$^+$, 91 (58) [C$_7$H$_7$]$^+$. MS (20 eV, EI): m/z (%) = 415 (6) [M + 2]$^+$, 413 (9) [M]$^+$, 276 (9) [P(O)(OH)(NHCH$_2$C$_6$H$_5$)$_2$]$^+$, 275 (8) [P(O)(O)(NHCH$_2$C$_6$H$_5$)$_2$]$^+$, 141 (9) [4-^{37}Cl-C$_6$H$_4$CO]$^+$, 139 (34) [4-^{35}Cl-C$_6$H$_4$CO]$^+$, 137 (75) [4-^{35}Cl-C$_6$H$_4$CN]$^+$, 106 (100) [C$_7$H$_8$N]$^+$, 91 (81) [C$_7$H$_7$]$^+$.

3: M.p. 226 °C. Anal. Calc. for $C_{21}H_{21}ClN_3O_2P$ (%): C = 60.95; H = 5.11; N = 10.15; found: C = 61.32; H = 5.02; N = 10.47. $^{31}P\{^1H\}$ NMR (DMSO-d_6): δ = −4.57 (s). ^1H NMR (DMSO-d_6): δ = 2.17 (s, 6H, Me), 6.97 (d, ^3J(H,H) = 8.1 Hz, 4H), 7.07 (d, ^3J(H,H) = 8.3 Hz, 4H), 7.52 (d, ^3J(H,H) = 8.5 Hz, 2H), 7.77 (d, ^2J(P,H) = 9.8 Hz, 2H, NH), 7.94 (d, ^3J(H,H) = 8.5 Hz, 2H), 10.00 (d, ^2J(P,H) = 7.9 Hz, 1H, NH). $^{13}C\{^1H\}$ NMR (DMSO-d_6): δ = 20.23, 117.81 (d, ^2J(P,C) = 7.3 Hz), 128.47, 129.21, 130.09, 132.05 (d, ^3J(P,C) = 8.8 Hz), 166.87. IR (KBr, cm^{-1}): 3293, 3067, 2870, 2730, 1884, 1653, 1591, 1514, 1440, 1386, 1275, 1224, 1111, 1011, 960, 882, 816, 748, 680. MS (70 eV, EI): m/z (%) = 415 (1) [M + 2]$^+$, 413 (6) [M]$^+$, 412 (2) [M − 1]$^+$, 141 (5) [4-^{37}Cl-C$_6$H$_4$CO]$^+$, 139 (44) [4-^{35}Cl-C$_6$H$_4$CO]$^+$, 137 (10) [4-^{35}Cl-C$_6$H$_4$CN]$^+$, 107 (100) [C$_7$H$_9$N]$^+$, 106 (82) [C$_7$H$_8$N]$^+$, 92 (3) [C$_7$H$_8$]$^+$. MS (20 eV, EI): m/z (%) = 415 (1) [M + 2]$^+$, 413 (4) [M]$^+$, 276 (9) [P(O)(OH)(NHC$_6$H$_4$-4-CH$_3$)$_2$]$^+$, 141 (5) [4-^{37}Cl-C$_6$H$_4$CO]$^+$, 139 (43) [4-^{35}Cl-C$_6$H$_4$CO]$^+$, 137 (92) [4-^{35}Cl-C$_6$H$_4$CN]$^+$, 106 (100) [C$_7$H$_8$N]$^+$, 92 (4) [C$_7$H$_8$]$^+$.

4: M.p. 145 °C. Anal. Calc. for $C_{23}H_{25}FN_3O_2P$ (%): C = 64.93; H = 5.92; N = 9.88; found: C = 64.23; H = 5.76; N = 10.24. $^{31}P\{^1H\}$ NMR (DMSO-d_6): δ = 14.44 (s). ^{19}F NMR (DMSO-d_6): δ = −113.06 (m). ^1H NMR

(DMSO-d_6): δ = 2.55 (d, ^3J(P,H) = 10.1 Hz, 6H, Me), 4.17 (dd, ^3J(P,H) = 9.2 Hz, ^2J(H,H) = 15.1 Hz, 2H, CH$_{Bz}$), 4.24 (dd, ^3J(P,H) = 9.2 Hz, ^2J(H,H) = 15.1 Hz, 2H, CH$_{Bz}$), 7.23 (t, ^3J(H,H) = 7.3 Hz, 2H), 7.30 (t, ^3J(H,H) = 7.5 Hz, 4H), 7.40 (d, ^3J(H,H) = 7.4 Hz, 4H), 7.43 (dt, ^3J[(H,H), (F,H)] = 8.5 Hz, ^4J(H,H) = 2.3 Hz, 1H), 7.52 (dt, ^3J(H,H) = 7.9 Hz, ^4J(F,H) = 6.0 Hz, 1H), 7.79 (dd, ^3J(F,H) = 9.8 Hz, ^4J(H,H) = 2.0 Hz, 1H), 7.82 (d, ^3J(H,H) = 7.8 Hz, 1H), 9.73 (s, 1H, NH). ^{13}C{^{1}H} NMR (DMSO-d_6): δ = 33.44 (d, ^2J(P,C) = 4.6 Hz), 52.06 (d, ^2J(P,C) = 5.1 Hz), 115.01 (d, ^2J(F,C) = 23.0 Hz), 119.10 (d, ^2J(F,C) = 21.2 Hz), 124.45 (d, ^4J(F,C) = 2.2 Hz), 126.99, 127.95, 128.24, 130.46 (d, ^3J(F,C) = 7.8 Hz), 135.98 (t, ^3J[(P,C), (F,C)] = 8.1 Hz), 138.21 (d, ^3J(P,C) = 4.0 Hz), 161.82 (d, ^1J(F,C) = 244.5 Hz), 167.23. IR (KBr, cm^{-1}): 3075, 2983, 2903, 1681, 1588, 1495, 1451, 1366, 1304, 1279, 1205, 1183, 1129, 1069, 1007, 943, 906, 894, 870, 794, 751, 729, 703, 596, 554, 524, 500, 474. MS (70 eV, EI): m/z (%) = 425 (44) [M]$^+$, 123 (26) [3-F-C$_6$H$_4$CO]$^+$, 121 (40) [3-F-C$_6$H$_4$CN]$^+$, 120 (81) [C$_8$H$_{10}$N]$^+$, 43 (44) [C$_2$H$_5$N]$^+$, 29 (100) [CH$_3$N]$^+$. MS (20 eV, EI): m/z (%) = 425 (1) [M]$^+$, 304 (< 1) [P(O)(OH)[N(CH$_3$)(CH$_2$C$_6$H$_5$)]$_2$]$^+$, 303 (< 1) [P(O)(O)[N(CH$_3$)(CH$_2$C$_6$H$_5$)]$_2$]$^+$, 123 (4) [3-F-C$_6$H$_4$CO]$^+$, 121 (57) [3-F-C$_6$H$_4$CN]$^+$, 120 (9) [C$_8$H$_{10}$N]$^+$, 43 (100) [C$_2$H$_5$N]$^+$.

5: M.p. 136 °C. Anal. Calc. for C$_{23}$H$_{24}$F$_2$N$_3$O$_2$P (%): C = 62.30; H = 5.45; N = 9.48; found: C = 61.38; H = 5.32; N = 10.31. ^{31}P{^{1}H} NMR (DMSO-d_6): δ = 14.23 (s). ^{19}F NMR (DMSO-d_6): δ = –109.22 (m). ^{1}H NMR (DMSO-d_6): δ = 2.54 (d, ^3J(P,H) = 10.2 Hz, 6H, Me), 4.16 (dd, ^3J(P,H) = 9.2 Hz, ^2J(H,H) = 15.1 Hz, 2H, CH$_{Bz}$), 4.23 (dd, ^3J(P,H) = 9.2 Hz, ^2J(H,H) = 15.1 Hz, 2H, CH$_{Bz}$), 7.23 (t, ^3J(H,H) = 7.3 Hz, 2H), 7.30 (t, ^3J(H,H) = 7.5 Hz, 4H), 7.39 (d, ^3J(H,H) = 7.3 Hz, 4H), 7.51 (tt, ^3J(F,H) = 9.0 Hz, ^4J(H,H) = 2.4 Hz, 1H), 7.67 (m, 2H), 9.71 (s, 1H, NH). ^{13}C{^{1}H} NMR (DMSO-d_6): δ = 33.45 (d, ^2J(P,C) = 4.7 Hz), 52.02 (d, ^2J(P,C) = 5.0 Hz), 107.69 (t, ^2J(F,C) = 25.9 Hz), 111.66 (dd, ^2J(F,C) = 20.6 Hz, ^4J(F,C) = 6.4 Hz), 127.03, 127.96, 128.26, 137.03 (m), 138.15 (d, ^3J(P,C) = 4.0 Hz), 162.10 (dd, ^1J(F,C) = 247.4 Hz, ^3J(F,C) = 12.7 Hz), 165.98. IR (KBr, cm^{-1}): 3096, 2910, 1685, 1595, 1485, 1443, 1324, 1177, 1115, 1006, 854, 792, 750, 692. MS (70 eV, EI): m/z (%) = 443 (22) [M]$^+$, 141 (11) [3,5-F$_2$-C$_6$H$_3$CO]$^+$, 139 (< 1) [3,5-F$_2$-C$_6$H$_3$CN]$^+$, 120 (98) [C$_8$H$_{10}$N]$^+$, 119 (100) [C$_8$H$_9$N]$^+$, 91 (98) [C$_7$H$_7$]$^+$, 43 (68) [C$_2$H$_5$N]$^+$, 29 (98) [CH$_3$N]$^+$. MS (20 eV, EI): m/z (%) = 443 (2) [M]$^+$, 442 (< 1) [M − 1]$^+$, 304 (< 1) [P(O)(OH)[N(CH$_3$)(CH$_2$C$_6$H$_5$)]$_2$]$^+$, 303 (< 1) [P(O)(O)[N(CH$_3$)(CH$_2$C$_6$H$_5$)]$_2$]$^+$, 141 (2) [3,5-F$_2$-C$_6$H$_3$CO]$^+$, 139 (3) [3,5-F$_2$-C$_6$H$_3$CN]$^+$, 120 (4) [C$_8$H$_{10}$N]$^+$, 91 (12) [C$_7$H$_7$]$^+$, 59 (100) [N$_2$P]$^+$, 43 (45) [C$_2$H$_5$N]$^+$.

6: M.p. 156 °C. Anal. Calc. for C$_{12}$H$_{16}$F$_2$N$_3$O$_2$P (%): C = 47.53; H = 5.32; N = 13.86; found: C = 47.13; H = 5.30; N = 14.45. ^{31}P{^{1}H} NMR (DMSO-d_6): δ = 1.57 (s). ^{19}F NMR (DMSO-d_6): δ = –109.38 (m). ^{1}H NMR (DMSO-d_6): δ = 0.77 (s, 3H, Me), 1.09 (s, 3H, Me), 2.58 (dd, ^3J(P,H) = 26.2 Hz, ^2J(H,H) = 11.8 Hz, 2H, CH$_{equatorial}$), 3.03 (d, ^2J(H,H) = 11.8 Hz, 2H, CH$_{axial}$), 4.62 (br. s, 2H, NH), 7.48 (t, ^3J(H,F) = 9.0 Hz, 1H), 7.68 (m, 2H), 9.43 (d, ^2J(P,H) = 7.3 Hz, 1H, NH). ^{13}C{^{1}H} NMR (DMSO-d_6): δ = 23.00, 24.77, 30.16 (d, ^3J(P,C) = 5.0 Hz), 53.11 (d, ^2J(P,C) = 1.8 Hz), 107.35 (t, ^2J(F,C) = 26.0 Hz), 111.35 (dd, ^2J(F,C) = 20.5 Hz, ^4J(F,C) = 6.3 Hz), 137.30 (m), 162.13 (dd, ^1J(F,C) = 247.2 Hz, ^3J(F,C) = 12.6 Hz), 166.07. IR (KBr,

cm^{-1}): 3353, 3262, 3066, 2961, 1673, 1596, 1444, 1315, 1186, 1109, 985, 952, 866, 761. MS (70 eV, EI): m/z (%) = 303 (8) [M]$^+$, 302 (40) [M – 1]$^+$, 141 (100) [3,5-F$_2$-C$_6$H$_3$CO]$^+$, 139 (6) [3,5-F$_2$-C$_6$H$_3$CN]$^+$, 100 (6) [C$_5$H$_{12}$N$_2$]$^+$, 71 (46) [C$_5$H$_{11}$]$^+$, 42 (35) [C$_3$H$_6$]$^+$. MS (20 eV, EI): m/z (%) = 303 (5) [M]$^+$, 302 (3) [M – 1]$^+$, 164 (9) [M – 3,5-F$_2$-C$_6$H$_3$CN]$^+$, 141 (6) [3,5-F$_2$-C$_6$H$_3$CO]$^+$, 139 (8) [3,5-F$_2$-C$_6$H$_3$CN]$^+$, 121 (100) [C$_7$H$_2$FO]$^+$, 100 (2) [C$_5$H$_{12}$N$_2$]$^+$, 71 (3) [C$_5$H$_{11}$]$^+$, 42 (15) [C$_3$H$_6$]$^+$.

7: M.p. 132 °C. Anal. Calc. for C$_{23}$H$_{24}$F$_2$N$_3$O$_2$P (%): C = 62.30; H = 5.45; N = 9.48; found: C = 62.44; H = 5.44; N = 9.65. ^{31}P{^{1}H} NMR (DMSO-d$_6$): δ = 12.96 (s). ^{19}F NMR (DMSO-d$_6$): δ = –139.80 (dt, ^3J(F,F) = 23.2 Hz, ^4J(H,F) = 7.0 Hz), –138.31 (ddd, ^3J(F,F) = 23.2 Hz, ^3J(H,F) = 11.0 Hz, ^4J(H,F) = 4.7 Hz). ^{1}H NMR (DMSO-d$_6$): δ = 2.54 (d, ^3J(P,H) = 10.2 Hz, 6H, Me), 4.17 (dd, ^2J(H,H) = 15.2 Hz, ^3J(P,H) = 8.6 Hz, 2H, CH$_{Bz}$), 4.24 (dd, ^2J(H,H) = 15.2 Hz, ^3J(P,H) = 9.3 Hz, 2H, CH$_{Bz}$), 7.24 – 7.28 (m, 2H), 7.28 – 7.32 (m, 1H), 7.34 (t, ^3J(H,H) = 7.6 Hz, 4H), 7.37 (tdd, ^3J(H,H) = 7.4 Hz, ^4J(F,H) = 5.7 Hz, ^5J(F,H) = 1.4 Hz, 1H), 7.39 – 7.43 (m, 4H), 7.56 – 7.64 (m, 1H), 9.81 (br. s, 1H, NH). ^{13}C{^{1}H} NMR (DMSO-d$_6$): δ = 33.31 (d, ^2J(P,C) = 4.6 Hz), 51.96 (d, ^2J(P,C) = 4.8 Hz), 119.84 (d, ^2J(F,C) = 17.2 Hz), 124.70 (m), 124.91 (dd, ^3J(F,C) = 6.9 Hz, ^4J(F,C) = 4.4 Hz), 126.45 (dd, ^2J(F,C) = 11.7 Hz, ^3J(P,C) = 9.1 Hz), 127.13, 128.00, 128.37, 138.18 (d, ^3J(P,C) = 4.4 Hz), 147.19 (dd, ^1J(F,C) = 251.3 Hz, ^2J(F,C) = 13.8 Hz), 149.62 (dd, ^1J(F,C) = 246.7 Hz, ^2J(F,C) = 12.7 Hz), 165.13 (t, J = 2.6 Hz). IR (KBr, cm^{-1}): 3065, 2892, 1679, 1588, 1483, 1454, 1348, 1296, 1195, 1137, 1008, 950, 854, 797, 696. MS (70 eV, EI): m/z (%) = 443 (90) [M]$^+$, 442 (88) [M – 1]$^+$, 141 (2) [2,3-F$_2$-C$_6$H$_3$CO]$^+$, 139 (42) [2,3-F$_2$-C$_6$H$_3$CN]$^+$, 120 (80) [C$_8$H$_{10}$N]$^+$, 119 (100) [C$_8$H$_9$N]$^+$, 91 (80) [C$_7$H$_7$]$^+$. MS (20 eV, EI): m/z (%) = 443 (12) [M]$^+$, 304 (< 1) [P(O)(OH)[N(CH$_3$)(CH$_2$C$_6$H$_5$)]$_2$]$^+$, 303 (< 1) [P(O)(O)[N(CH$_3$)(CH$_2$C$_6$H$_5$)]$_2$]$^+$, 141 (10) [2,3-F$_2$-C$_6$H$_3$CO]$^+$, 139 (7) [2,3-F$_2$-C$_6$H$_3$CN]$^+$, 120 (100) [C$_8$H$_{10}$N]$^+$, 91 (35) [C$_7$H$_7$]$^+$.

8: M.p. 165 °C. Anal. Calc. for C$_{23}$H$_{25}$ClN$_3$O$_2$P (%): C = 62.52; H = 5.70; N = 9.51; found: C = 62.80; H = 5.65; N = 9.53. ^{31}P{^{1}H} NMR (122 MHz, DMSO-d$_6$): δ = 4.49 (s). ^{1}H NMR (301 MHz, DMSO-d$_6$): δ = 1.40 (apparent-t, ^3J(H,H) = 6.3 Hz, 6H, CH$_3$), 4.36 (m, 2H, CH), 4.87 (t, J = 10.2 Hz, 1H, NH), 4.97 (t, J = 10.2 Hz, 1H, NH), 7.12 – 7.50 (m, 14H, Ar–H), 8.95 (br. s, 1H, NH). ^{13}C{^{1}H} NMR (76 MHz, DMSO-d$_6$): δ = 25.75 (d, ^3J(P,C) = 5.0 Hz), 26.11 (d, ^3J(P,C) = 6.6 Hz), 50.22, 50.42, 126.49, 126.57, 126.77, 127.20, 127.32, 128.48, 129.00, 129.56, 130.06, 130.25, 131.50, 136.68 (d, ^3J(P,C) = 8.9 Hz), 146.60 (d, ^3J(P,C) = 4.5 Hz), 146.82 (d, ^3J(P,C) = 5.8 Hz), 168.40 (d, ^2J(P,C) = 1.7 Hz). IR (KBr, cm^{-1}): 3242, 3060, 3030, 2968, 2923, 1804, 1663, 1593, 1556, 1478, 1428, 1291, 1249, 1196, 1121, 1064, 974, 889, 855, 812, 749, 698. MS (70 eV, EI): m/z (%) = 443 (56) [M + 2]$^+$, 441 (83) [M]$^+$, 287 (28) [M – C$_7$H$_5$^{35}ClNO]$^+$, 154 (70) [C$_7$H$_5$^{35}ClNO]$^+$, 139 (54) [C$_7$H$_4$^{35}ClO]$^+$, 137 (81) [2-^{35}Cl-C$_6$H$_4$CN]$^+$, 120 (88) [C$_8$H$_{10}$N]$^+$, 106 (100) [C$_8$H$_{10}$]$^+$. MS (20 eV, EI): m/z (%) = 443 (<1) [M + 2]$^+$, 441 (2) [M]$^+$, 304 (1) [M – 2-^{35}Cl-C$_6$H$_4$CN]$^+$, 141 (12) [C$_7$H$_4$^{37}ClO]$^+$, 139 (57) [C$_7$H$_4$^{35}ClO]$^+$, 137 (91) [2-^{35}Cl-C$_6$H$_4$CN]$^+$, 120 (91) [C$_8$H$_{10}$N]$^+$, 106 (100) [C$_8$H$_{10}$]$^+$.

9: M.p. 165 °C. Anal. Calc. for $C_{23}H_{25}ClN_3O_2P$ (%): C = 62.52; H = 5.70; N = 9.51; found: C = 61.34; H = 5.53; N = 9.50. $^{31}P\{^1H\}$ NMR (122 MHz, CDCl$_3$): δ = 5.03 (s). ^1H NMR (301 MHz, CDCl$_3$): δ = 1.37 (d, ^3J(H,H) = 6.9 Hz, CH$_3$), 1.51 (d, ^3J(H,H) = 6.9 Hz, CH$_3$), 3.50 (t, J = 9.4 Hz, 1H, NH), 3.76 (t, J = 9.4 Hz, 1H, NH), 4.52 (m, 2H, CH), 7.14 – 7.38 (m, 14H, Ar–H), 8.61 (br. s, 1H, NH). $^{13}C\{^1H\}$ NMR (76 MHz, CDCl$_3$): δ = 25.22 (d, ^3J(P,C) = 2.0 Hz), 25.31 (d, ^3J(P,C) = 4.0 Hz), 50.64, 51.93, 125.90, 125.99, 126.12, 126.83, 126.96, 127.08, 128.48, 128.62, 130.04, 130.43, 131.92, 133.90 (d, ^3J(P,C) = 8.2 Hz), 144.84 (d, ^3J(P,C) = 3.7 Hz), 145.14 (d, ^3J(P,C) = 5.3 Hz), 168.19 (d, ^2J(P,C) = 1.9 Hz). IR (KBr, cm^{-1}): 3237, 3063, 2972, 2917, 1744, 1664, 1593, 1430, 1289, 1201, 1118, 1080, 1045, 977, 893, 859, 817, 749, 701. MS (70 eV, EI): m/z (%) = 443 (26) [M + 2]$^+$, 441 (67) [M]$^+$, 304 (< 1) [M – 2-^{35}Cl-C$_6$H$_4$CN]$^+$, 287 (3) [M – C$_7$H$_5$^{35}ClNO]$^+$, 154 (8) [C$_7$H$_5$^{35}ClNO]$^+$, 139 (18) [C$_7$H$_4$^{35}ClO]$^+$, 137 (55) [2-^{35}Cl-C$_6$H$_4$CN]$^+$, 120 (64) [C$_8$H$_{10}$N]$^+$, 119 (100) [C$_8$H$_9$N]$^+$. MS (20 eV, EI): m/z (%) = 443 (< 1) [M + 2]$^+$, 441 (< 1) [M]$^+$, 141 (12) [C$_7$H$_4$^{37}ClO]$^+$, 139 (32) [C$_7$H$_4$^{35}ClO]$^+$, 137 (66) [2-^{35}Cl-C$_6$H$_4$CN]$^+$, 120 (49) [C$_8$H$_{10}$N]$^+$, 106 (100) [C$_8$H$_{10}$]$^+$.

Spectroscopic features of new phosphoric triamides
Mass spectrometry analysis

Molecular ions for all nine compounds are revealed in the mass spectra, at m/z of 593/595, 413/415, 413/415, 441/443 and 441/443 (related to the ^{35}Cl/^{37}Cl isotopes) for **1**, **2**, **3**, **8** and **9** and at 425, 443, 303 and 443 for **4** – **7**, respectively.

A previous paper about mass spectra of [C$_6$H$_5$C(O)NH]P(O)[NR^1R^2]$_2$ phosphoramides discussed on a fragmentation pathway yielding phenylcyanide radical-cation, formed by removal of the related neutral (HO)P(O)[NR^1R^2]$_2$ amidophosphoric acid. This fragmentation involves an intramolecular re-arrangement done by a migration of phosphorus from nitrogen to oxygen (Gholivand *et al*., 2007). The mass spectra of compounds reported here confirm the previously reported mechanism by detecting chloro-, fluoro- and difluoro- derivatives of phenylcyanide radical-cation in both 20 and 70 eV experiments. The peaks resulting from the amidophosphoric acid radical-cations are also detected in the 20 eV experiments (demonstrating the charge could appear alternatively on either fragment); however, considerably lower intensities of the amidophosphoric acid radical-cations propose that this second pathway is not preferred. The peaks at m/z of 137 for **1/2/3** and **8/9**, at 121 for **4**, at 139 for **5/6** and **7** are related to the 4-chloro-, 2-chloro- (^{35}Cl isotope), 3-fluoro-, 3,5-difluoro- and 2,3-difluoro- derivatives of phenylcyanide radical-cations, respectively. The lowest relative intensities are observed for the 3,5-difluoro-phenylcyanide radical-cations in both experiments with respect to the other substituted phenylcyanide radical-cations studied here.

IR spectroscopy

For compounds **1**, **4**, **5** and **7**, the unique NH unit (of the C(O)NHP(O) segment) takes part in the N$_{CP}$—H…O═P hydrogen bond, while for compounds **2**, **3**, **8** and **9** (including three NH units) the N—H…O═P and N—H…O═C hydrogen bonds are present in the solid state (supported by X-ray crystallography

experiments). So, the relatively lower C=O stretching vibrations frequencies for **2**, **3**, **8** and **9** (1652 cm^{-1} (Dehghanpour *et al.*, 2010), 1653 cm^{-1}, 1663 cm^{-1} and 1664 cm^{-1}, respectively) with respect to the ones for **1**, **4**, **5** and **7** (1666 cm^{-1} (Dehghanpour *et al.*, 2010), 1681 cm^{-1}, 1685 cm^{-1} and 1679 cm^{-1}, respectively) are related to the involvement of C=O groups in the hydrogen bonds. Surprisingly, although compound **6** includes three NH units, but the C=O group does not take part in the hydrogen bonding interaction, while it shows the [N_{CP}—H…][N_P—H…][N_P—H…]O=P hydrogen bond in the solid state (supported by X-ray crystallography). So, the C=O stretching mode appears at the higher frequency (of 1673 cm^{-1}) with respect to the ones for compounds **2**, **3**, **8** and **9**.

NMR spectroscopy

^{1}HNMR

In the ^{1}HNMR spectra (in DMSO-d$_6$ for **1** to **8** and in CDCl$_3$ for **9**), the broad signals at 9.91, 9.40, 9.81, 8.95 and 8.61 ppm for **1**, **2**, **7**, **8** and **9**, respectively, and the doublet signals at 10.00 ppm for **3** (^2J(P,H) = 7.9 Hz) and at 9.43 ppm for **6** (^2J(P,H) = 7.3 Hz) and the singlet peaks at 9.73 and 9.71 ppm for **4** and **5** (respectively) are related to the N_{CP}—H protons. The compounds **2**, **3**, **6**, **8** and **9** contain two other NH units and the multiplet at 5.04 ppm for **2** (due to splitting with CH$_2$ protons and P atom), doublet at 7.77 ppm for **3** (^2J(P,H) = 9.8 Hz), broad singlet at 4.62 ppm for **6**, triplets at 4.87 ppm and 4.97 ppm (both J = 10.2 Hz) for **8** and triplets at 3.50 ppm and 3.76 ppm (both J = 9.4 Hz) for **9** associate to these protons. For **8** and **9**, fine structures for NH signals of amine fragments are related to the vicinal couplings with proton and phosphorus.

For the methyl protons in compounds **4**, **5** and **7**, doublet signals are revealed at 2.55, 2.54 and 2.54 ppm, respectively (J = 10.1, 10.2 and 10.2 Hz); the ^{31}P decoupling experiment for **7** demonstrates the coupling is due to the P atom nuclear spin (^3J(P,H)) (Figure S1). In the CH$_2$ group of **4**, **5** and **7**, the two H atoms are not equivalent and two dd signals (4.17/4.16/4.17 ppm and 4.24/4.23/4.24 ppm) are revealed due to geminal H-H (^2J(H,H) = 15.1 Hz for **4** and **5** and 15.2 Hz for **7**) and vicinal P-H (^3J(P,H) = 9.2 Hz for **4** and **5** and 8.6/9.3 Hz for **7**) couplings. The two protons are diastereotopic, surprisingly resulting in different ^3J(P,H) values for **7**. After decoupling of ^{31}P nucleus for **7**, two doublets are revealed (Figure S1).

In the ^{1}H NMR spectrum of compound **6**, the protons of two methyl groups appear at 0.77 and 1.09 ppm. Furthermore, the two signals at 2.58 and 3.03 ppm are related to the two protons of the CH$_2$ group in the diazaphosphorinane ring. The first signal appears as a dd due to the geminal H-H and vicinal P-H couplings (^2J(H,H) = 11.8 Hz, ^3J(P,H) = 26.2 Hz), whereas, the second signal appears as a doublet (^2J(H,H) = 11.8 Hz) and does not show the coupling arisen from the P nucleus. This difference is due to the spatial positions of H$_{axial}$ and H$_{equatorial}$ with respect to phosphorus, which can be shown by different torsion angles H$_{axial}$—C—N—P and H$_{equatorial}$—C—N—P, causing to the different hydrogen-phosphorus coupling

constants similar to what were reported for ^3J(H,H) coupling constants in the H—C—C—H systems and their dependency to the H—C—C—H torsion angles according to the Karplus equation (Drago, 1992). Moreover, the high ^3J(P,H) value for one proton and not observing the ^3J(P,H) value for the other proton is a result of the relatively fix environment in the CH_2—NH—P system within the ring. Such a system (CH_2—NH—P) in the acyclic situation, for example in compound **2**, showed the lower coupling constant which is an averaged value of two coupling constants due to the rotation around C—N and N—P bonds. The triplet signal at 7.48 ppm (for **6**) is related to the H4 atom (^3J(H,F) = 9.0 Hz) (the labeling of H4 is according to Figure S7, i.e. the hydrogen attached to C4A/C4B in the molecular structure). The stereoisomers **8** and **9** were studied in different solvents; for compound **8** (in DMSO-d_6) the triplet at 1.40 ppm (J = 6.3 Hz) is related to two overlapped methyl groups' signals, and similar protons in compound **9** ($CDCl_3$) appear as doublet signals at 1.37 ppm and 1.51 ppm (both ^3J(H,H) = 6.9 Hz). The multiplets at 4.36 and 4.52 ppm belong to the CH-protons in **8** and **9**, respectively.

The fluorine-hydrogen and hydrogen-hydrogen couplings give rise to one "dd" and two "dt" signals in ^{1}H NMR spectrum of **4** (3-F-C_6H_4 substituent) and one "tt" and one multiplet in ^{1}H NMR spectrum of **5** (3,5-F_2-C_6H_3 substituent) with resolved ^nJ(F,H) (n = 3, 4 for **4** and 3 for **5**) coupling constants. Surprisingly, the ^4J(H,H) coupling constants are observed in these fluorinated aryls. For example the "tt" pattern in the ^{1}H NMR spectrum of **5** (at 7.51 ppm) is a result of coupling with two fluorine (^3J) and two hydrogen (^4J) atoms. The fluorinated aryl in compound **6** is similar to one in compound **5** and the fine structures for the related protons are similar, unless ^4J(H,H) was not detected for **6**.

For the recognition of the 2,3-F_2-C_6H_3 protons (compound **7**), the ^{19}F decoupling experiment was also applied. This experiment causes the change in all of the three signals in the aromatic region which have the integrations fitting with 1 proton for each signal (Figure S1). On the other hand, after the ^{19}F decoupling experiment of ^{1}H NMR spectrum the multiplet signal at 7.28 – 7.32 ppm changes to a doublet signal and both tdd and multiplet signals at 7.37 and 7.56 – 7.64 ppm (respectively) convert to signals, both with a dd pattern.

^{31}PNMR

The phosphorus signals of **1**, **2**, **4**, **5**, **6**, **7**, **8** and **9** are revealed at 15.71, 8.90, 14.44, 14.23, 1.57, 12.96, 4.49 and 5.03 ppm, respectively, while for **3**, it appears at a negative value of –4.57 ppm.

^{13}CNMR

In these compounds, the *ipso*-carbon atom bonded to the C=O group shows coupling with phosphorus; typical example is the doublet signal at 132.05 ppm for **3** (^3J(P,C) = 8.8 Hz). In fluorinated compounds, the coupling with fluorine is also observed; for example, a dd signal at 126.45 ppm (^2J(F,C) = 11.7 Hz and

^3J(P,C)= 9.1 Hz) is observed for compound **7** with the 2,3-F_2-C_6H_3C(O)NHP(O) segment [the assignment of the ^{13}C NMR was performed by running 2D HSQC experiment]. For compound **4**, the *ipso*-carbon atom noted appears as a triplet signal at 135.98 ppm (^3J(P,C) & ^3J(F,C) = 8.1 Hz), while for compounds **5** and **6**, their similar *ipso*-carbon atoms are revealed as multiplets at 137.03 and 137.30 ppm (respectively), arising from ^3J(F,C) couplings with two fluorine atoms and ^3J(P,C).

All five other carbon atoms of **4'** benzoyl group reveal as doublets due to the F-C couplings, from directly bonded fluorine-carbon (^1J(F,C) = 244.5 Hz) to fluorine-carbon with four bonds separation (^4J(F,C) = 2.2 Hz). Due to the symmetry of 3,5-diflouro benzoyl group (in **5** and **6**), in addition to the mentioned *ipso*-carbon, three other signals reveal for the five remaining carbon atoms: one triplet arisen from two ^2J couplings and two dd peaks (by ^1J and ^3J couplings for one signal and by ^2J and ^4J for the other).

For compound **7**, the signals at 124.91 ppm (dd) and at 124.70 ppm (m) are assigned to C7 and C6 (the labelling is according to Figure S8), respectively and the patterns of signals resulting from the effect of two fluorine atoms with three- and four-bond separations from the resonancing carbon atoms. The carbon atoms C3 and C4 (directly bonded to fluorine atoms) cause to the two doublet of doublets centered at 147.19 and 149.62 ppm (^1J(F,C) & ^2J(F,C) = 251.3 & 13.8 Hz and 246.7 & 12.7 Hz). For **1 – 9**, the carbonyl signals are revealed at 167.76, 167.12, 166.87, 167.23, 165.98, 166.07, 165.13, 168.40 and 168.19 ppm, respectively.
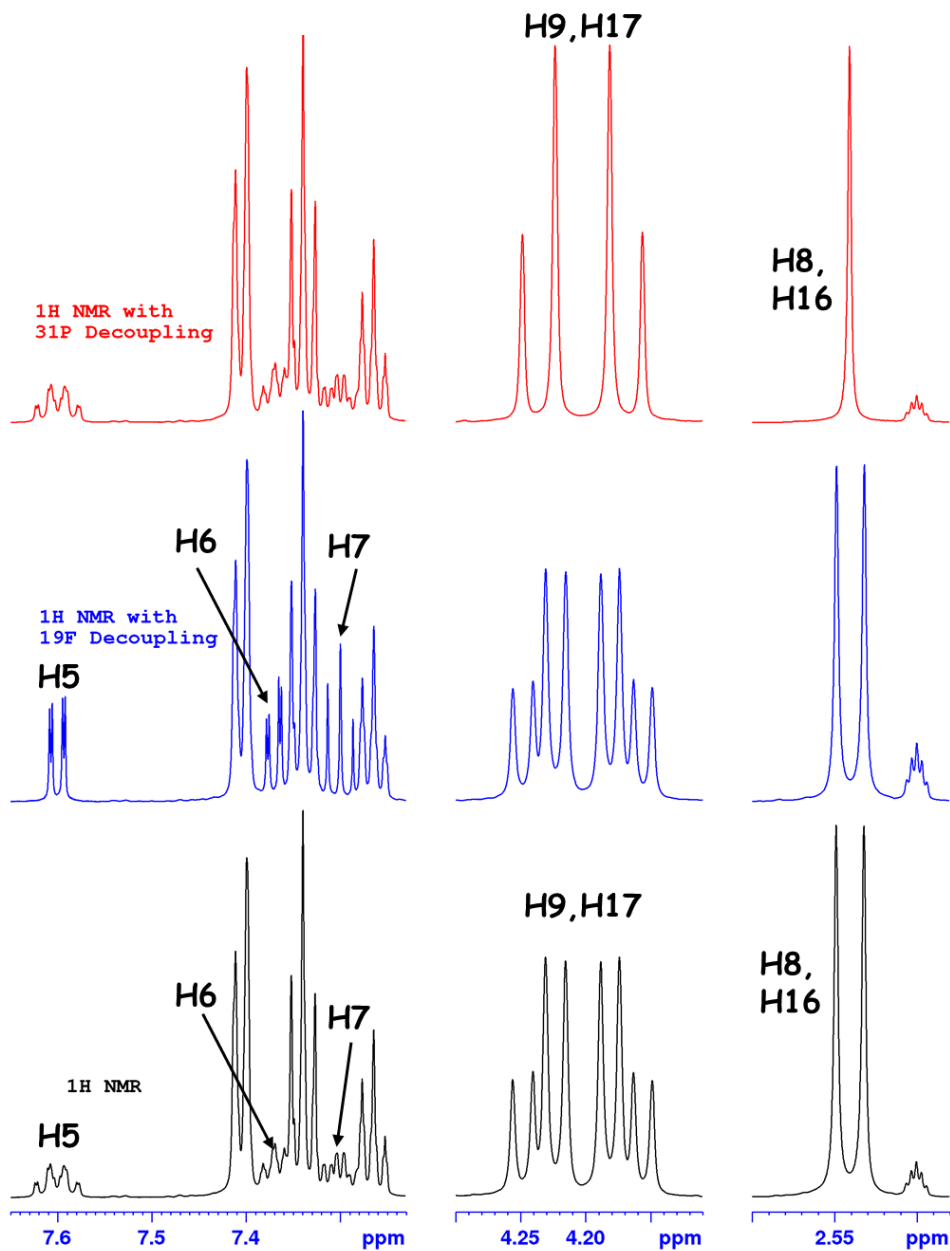
Figure S1. The effects of ^{31}P and ^{19}F decoupling experiments on the ^{1}H NMR spectrum of compound **7** are shown. The two $^{3}J(P,H)$ that cause multiplet structure for CH_2 (H9, H17) and doublet structure for CH_3 (H8, H16) protons could be resolved *via* ^{31}P decoupling of the ^{1}H NMR spectrum. Similraly, H5, H6 and H7 protons of the F_2-C_6H_3 group, which appear to be complex multiplets in the ^{1}H NMR spectrum, due to $^{3}J(F,H)$ and $^{4}J(F,H)$, could be well resolved *via* ^{19}F decoupling (for atom numbering refer to Figure S8).

Table S1. Selected bond distances (Å) and angles (°) for compounds **1** and **2**.

Compound **1**

P1-O1	1.4777 (14)	P2-N6	1.6446 (16)
P1-N1	1.6887 (16)	C1-N1	1.365 (2)
P1-N2	1.6403 (16)	C29-N2	1.480 (2)
P1-N3	1.6408 (17)	C22-N2	1.476 (2)
P2-O3	1.4762 (14)	C8-N3	1.477 (3)
P2-N4	1.6843 (17)	C1-O2	1.218 (2)
P2-N5	1.6420 (16)	C5-Cl1	1.739 (2)
O1-P1-N1	104.83 (8)	C8-N3-P1	119.45 (13)
O1-P1-N2	110.96 (8)	C15-N3-P1	121.66 (14)
O1-P1-N3	118.09 (9)	C15-N3-C8	114.74 (16)
N2-P1-N1	111.18 (8)	O3-P2-N4	105.39 (8)
N3-P1-N1	105.18 (9)	O3-P2-N5	110.59 (8)
N2-P1-N3	106.45 (8)	O3-P2-N6	118.62 (8)
C1-N1-P1	127.80 (14)	N5-P2-N4	111.95 (9)
C22-N2-P1	119.19 (12)	N6-P2-N4	104.43 (9)
C29-N2-P1	124.43 (13)	N5-P2-N6	105.81 (7)
Compound **2**			
P1-O1	1.4745(10)	N1-C1	1.3587(18)
P1-N1	1.7085(12)	N2-C8	1.4662(19)
P1-N2	1.6358(12)	N3-C15	1.4561(19)
P1-N3	1.6307(13)	Cl1-C5	1.7435(15)
O2-C1	1.2350(17)	C1-C2	1.494(2)
O1-P1-N1	105.18(6)	C1-N1-P1	120.63(10)
O1-P1-N2	117.01(6)	C8-N2-P1	121.16(10)
O1-P1-N3	114.06(6)	C15-N3-P1	123.26(10)
N2-P1-N1	108.55(6)	O2-C1-N1	119.52(13)
N3-P1-N1	110.49(6)	O2-C1-C2	119.92(13)
N3-P1-N2	110.53(6)	N1-C1-C2	120.56(12)

Table S2. Selected bond distances (Å) and angles (°) for compounds **3** and **4**.

Compound **3**			
P1-O1	1.4714 (10)	O2-C1	1.2296 (17)
P1-N1	1.6786 (13)	N1-C1	1.3682 (19)
P1-N2	1.6355 (14)	N2-C8	1.420 (2)
P1-N3	1.6366 (13)	N3-C15	1.409 (2)
O1-P1-N1	108.72 (6)	C1-N1-P1	123.83 (11)
O1-P1-N2	116.17 (7)	C8-N2-P1	128.20 (11)
O1-P1-N3	113.41 (7)	C15-N3-P1	127.11 (11)
N2-P1-N1	104.73 (7)	O2-C1-N1	119.79 (14)
N3-P1-N1	108.48 (7)	O2-C1-C2	121.10 (13)
N2-P1-N3	104.77 (7)	N1-C1-C2	119.10 (12)
Compound **4**			
P1-O2	1.4816 (10)	N1-C1	1.3718 (19)
P1-N1	1.6814 (12)	N2-C15	1.4601 (18)
P1-N2	1.6319 (13)	N3-C16	1.4666 (18)
P1-N3	1.6331 (12)	N3-C23	1.4674 (18)
O1-C1	1.2221 (17)	F1-C4	1.3630 (17)
O2-P1-N1	105.52 (6)	C15-N2-C8	114.73 (12)
O2-P1-N2	109.68 (6)	C15-N2-P1	125.80 (10)
O2-P1-N3	118.46 (6)	C8-N2-P1	119.47 (10)
N2-P1-N1	112.73 (7)	C16-N3-C23	113.59 (12)
N3-P1-N1	105.71 (6)	C16-N3-P1	125.74 (10)
N3-P1-N2	104.88 (6)	C23-N3-P1	118.16 (10)
C1-N1-P1	127.32 (12)	F1-C4-C5	118.66 (13)

Table S3. Selected bond distances (Å) and angles (°) for compounds **5** and **6**.

Compound **5**			
P1-O2	1.4788 (9)	N2-C14	1.4698(18)

P1-N1	1.6834 (11)	N2-C15	1.4691 (17)
P1-N2	1.6361 (12)	N3-C16	1.4612 (17)
P1-N3	1.6302 (11)	N3-C17	1.4623 (19)
O1-C7	1.2104 (17)	F2-C4	1.357 (2)
N1-C7	1.3669 (16)	C6-C7	1.5054 (18)
O2-P1-N1	104.75 (5)	C7-N1-P1	126.74 (9)
O2-P1-N2	119.04 (6)	C14-N2-C15	113.22 (12)
O2-P1-N3	109.92 (6)	C14-N2-P1	122.20 (9)
N2-P1-N1	105.86 (6)	C17-N3-C16	115.07 (11)
N3-P1-N1	112.55 (6)	C17-N3-P1	118.90 (9)
N2-P1-N3	104.85 (6)		
Compound **6**			
P1A-O2A	1.4777 (15)	P1B-O2B	1.4802 (15)
P1A-N1A	1.690 (2)	P1B-N1B	1.685 (2)
P1A-N2A	1.620 (2)	P1B-N2B	1.619 (2)
P1A-N3A	1.612 (2)	P1B-N3B	1.6125 (19)
N1A-C7A	1.364 (3)	N1B-C7B	1.368 (3)
N2A-C8A	1.460 (3)	N2B-C8B	1.460 (3)
N3A-C10A	1.462 (3)	N3B-C10B	1.465 (3)
F1A-C3A	1.355 (3)	F1B-C3B	1.353 (3)
F2A-C5A	1.352 (3)	F2B-C5B	1.350 (3)
O2A-P1A-N1A	104.56 (10)	O2B-P1B-N1B	104.63 (10)
O2A-P1A-N2A	114.75 (11)	O2B-P1B-N2B	115.31 (11)
O2A-P1A-N3A	113.96 (11)	O2B-P1B-N3B	113.83 (10)
N3A-P1A-N2A	103.07 (11)	N3B-P1B-N2B	103.64 (10)
N3A-P1A-N1A	110.89 (11)	N3B-P1B-N1B	110.56 (10)
N2A-P1A-N1A	109.73 (11)	N2B-P1B-N1B	108.91 (10)

Table S4. Selected bond distances (Å) and angles (°) for compounds **7**, **8** and **9**.

Compound **7**			
P1-O1	1.4756 (10)	N2-C8	1.4607 (18)
P1-N1	1.6866 (13)	N2-C9	1.4701 (19)
P1-N2	1.6353 (12)	N3-C17	1.4610 (19)
P1-N3	1.6331 (13)	N3-C16	1.467 (2)
O2-C1	1.2207 (17)	F1-C3	1.3452 (17)
N1-C1	1.3665 (19)	F2-C4	1.3540 (17)
O1-P1-N1	106.62 (6)	C8-N2-C9	114.57 (12)
O1-P1-N2	110.62 (6)	C8-N2-P1	123.63 (10)
O1-P1-N3	115.48 (6)	C9-N2-P1	121.79 (10)
N2-P1-N1	111.75 (6)	C17-N3-C16	114.58 (12)
N3-P1-N1	105.31 (6)	C17-N3-P1	127.21 (10)
N3-P1-N2	107.01 (6)	C16-N3-P1	117.58 (11)
C1-N1-P1	127.48 (11)		

Compound **8**

P1-O1	1.479 (3)	P1-N3	1.620 (3)
P1-N1	1.711 (2)	O2-C1	1.223 (4)
P1-N2	1.621 (2)	N1-C1	1.357 (4)
O1-P1-N1	103.07 (14)	N1-P1-N3	109.51 (12)
O1-P1-N2	115.74 (13)	N2-P1-N3	102.26 (16)
O1-P1-N3	115.75 (13)	P1-N1-C1	124.0 (2)
N1-P1-N2	110.60 (13)		

Compound **9**

P1-O1	1.480 (3)	P1-N3	1.623 (3)
P1-N1	1.708 (2)	O2-C1	1.217 (4)
P1-N2	1.624 (2)	N1-C1	1.366 (4)
O1-P1-N1	103.01 (15)	N1-P1-N3	109.23 (12)
O1-P1-N2	115.73 (13)	N2-P1-N3	102.40 (16)
O1-P1-N3	115.78 (13)	P1-N1-C1	123.6 (2)
N1-P1-N2	110.77 (13)		
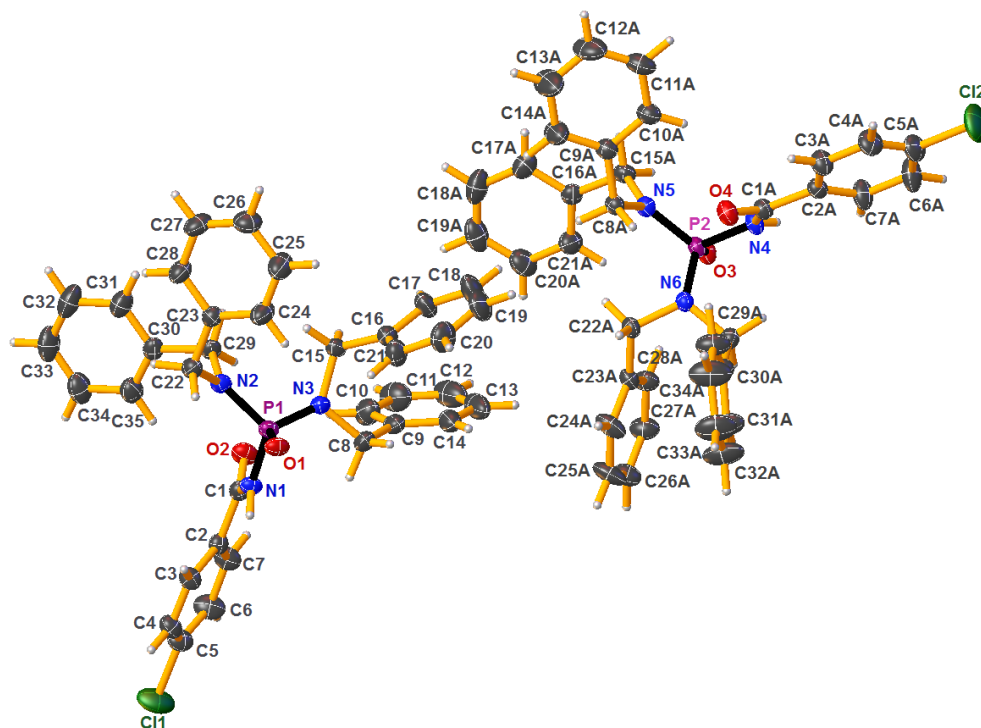
Figure S2. Displacement ellipsoid plot (30% probability) of the asymmetric unit of structure **1**, showing the atom numbering schemes. H atoms are drawn as spheres of arbitrary radii.
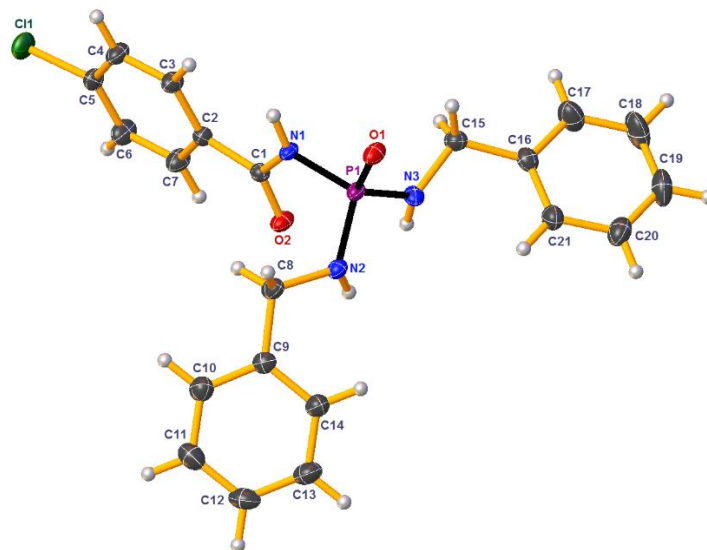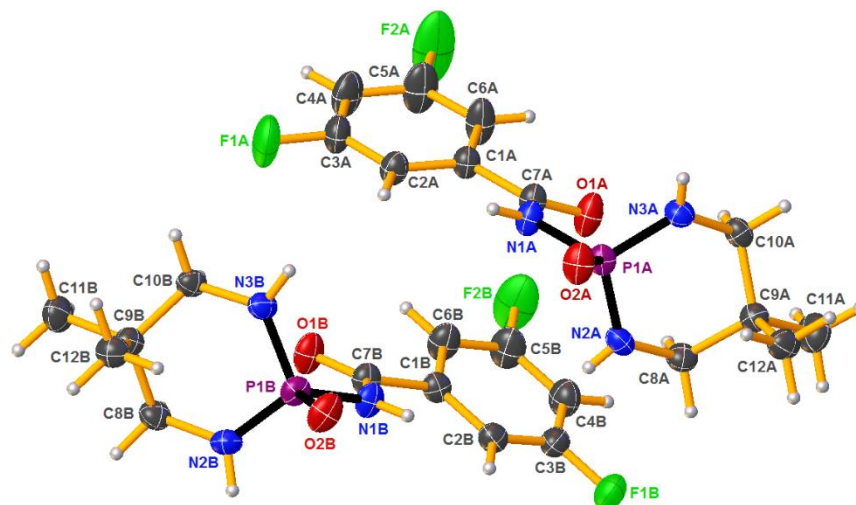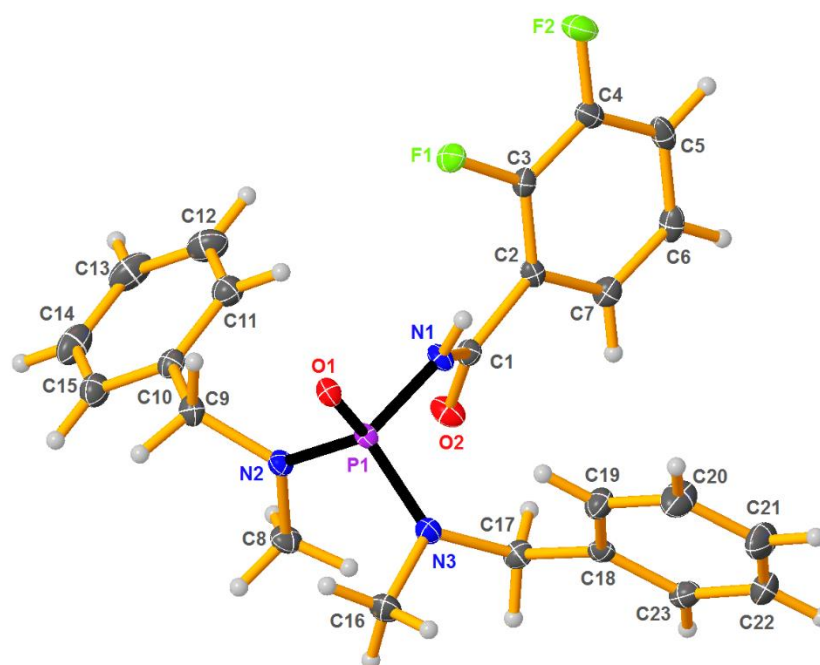
Figure S3. Displacement ellipsoid plot (50% probability) of **2** with atom numbering scheme. H atoms are drawn as spheres of arbitrary radii.
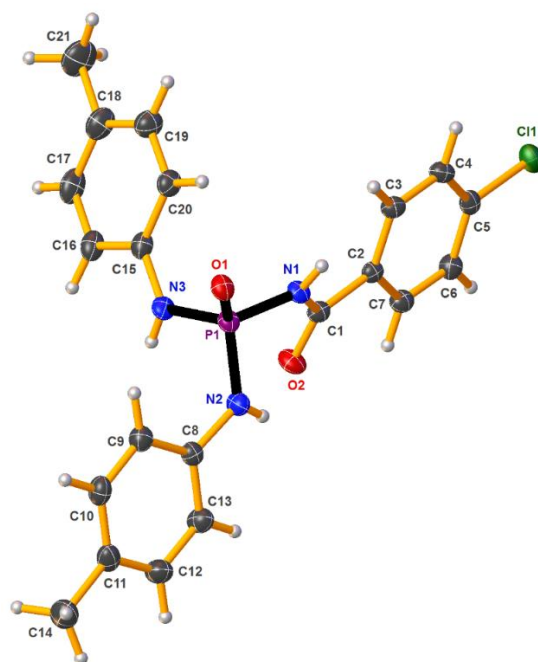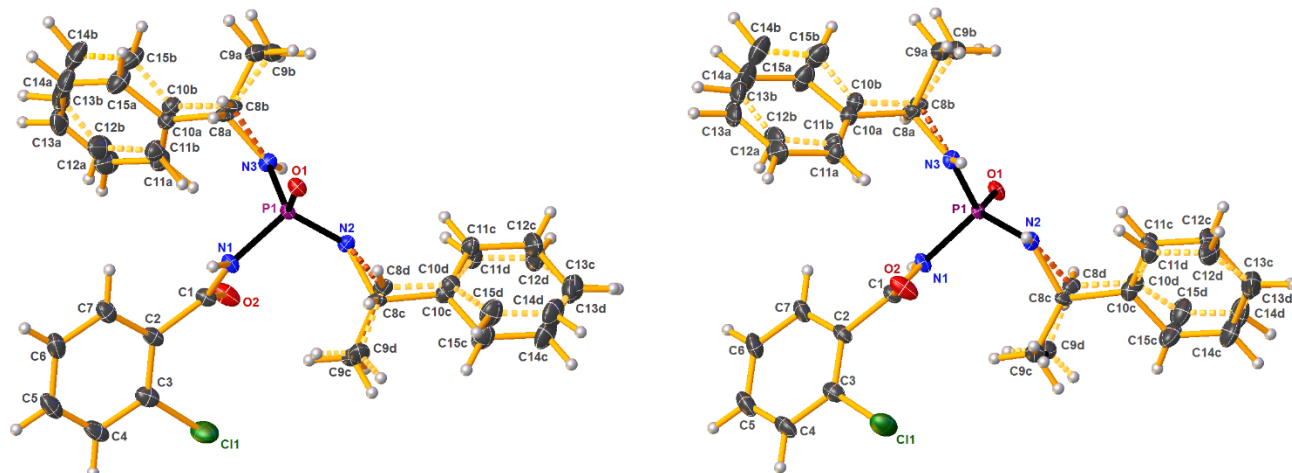

Figure S4. Displacement ellipsoid plot (50% probability) of **3** with atom numbering scheme. H atoms are drawn as spheres of arbitrary radii.
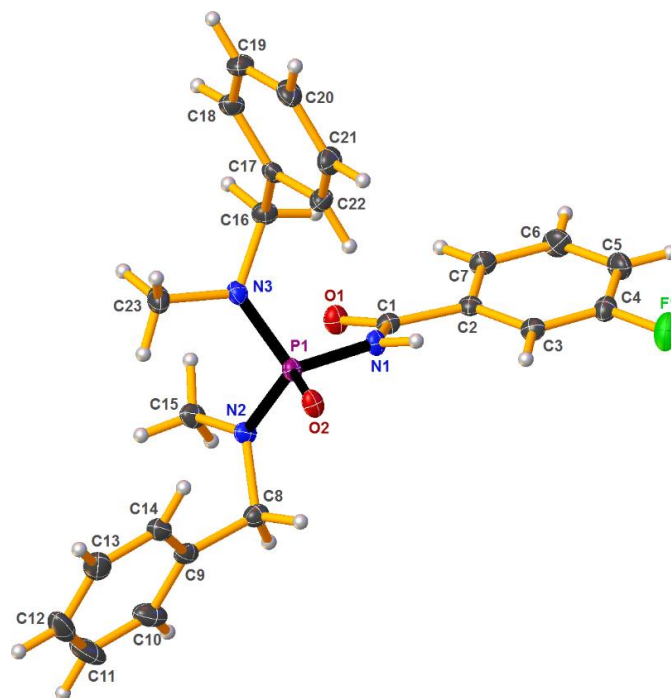
Figure S5. Displacement ellipsoid plot (50% probability) of **4** with atom numbering scheme. H atoms are drawn as spheres of arbitrary radii.
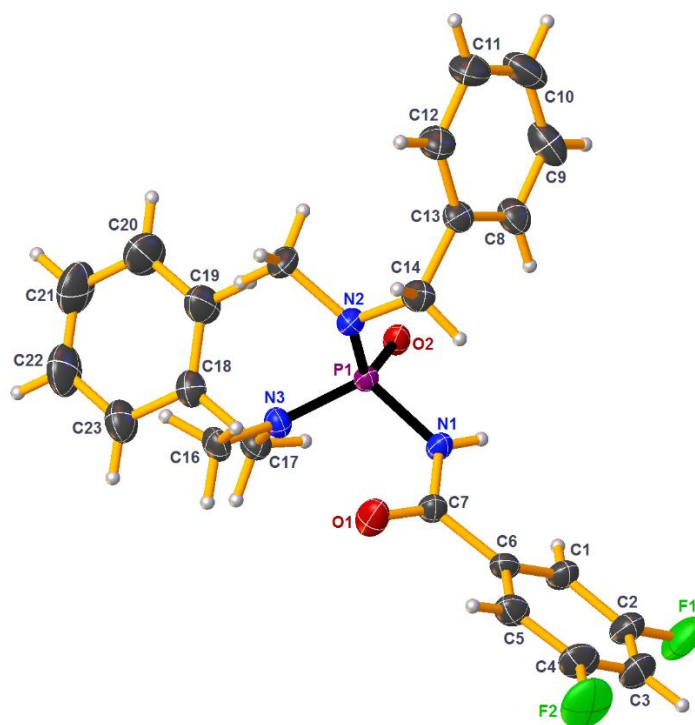
Figure S6. Displacement ellipsoid plot (50% probability) of **5** with atom numbering scheme. H atoms are drawn as spheres of arbitrary radii.

Figure S7. Displacement ellipsoid plot (50% probability) of **6** with atom numbering scheme. H atoms are drawn as spheres of arbitrary radii.

Figure S8. Displacement ellipsoid plot (50% probability) of **7** with atom numbering scheme. H atoms are drawn as spheres of arbitrary radii.

Figure S9. Displacement ellipsoid plots (50% probability) for **8** (left) and **9** (right), with atom-numbering scheme. H atoms are drawn as spheres of arbitrary radii. Dashed lines indicate the minor-disorder component.
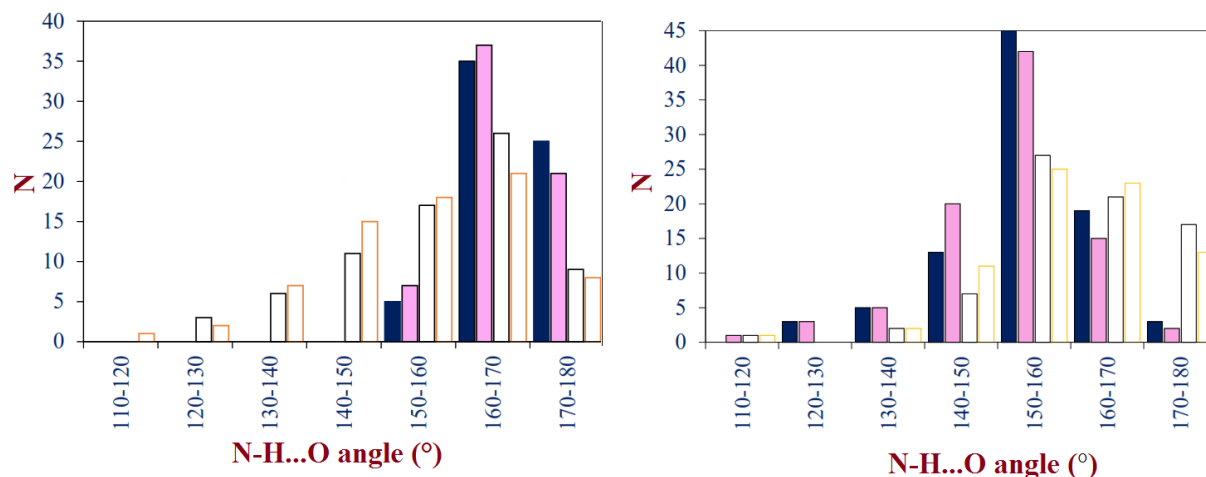
Figure S10. The histograms of N—H…O angles in $R_2^2(8)/R_2^2(12)$ (left) and $R_2^1(6)/R_2^2(10)$ (right) motifs of the $[RC(O)NH]P(O)[NHR^1]_2$ structures (in left histogram the hollow columns are related to the angles in $R_2^2(12)$ motifs as black frame (before) and orange frame (after) normalization. The dark blue and pink columns are related to the angles in $R_2^2(8)$ motifs b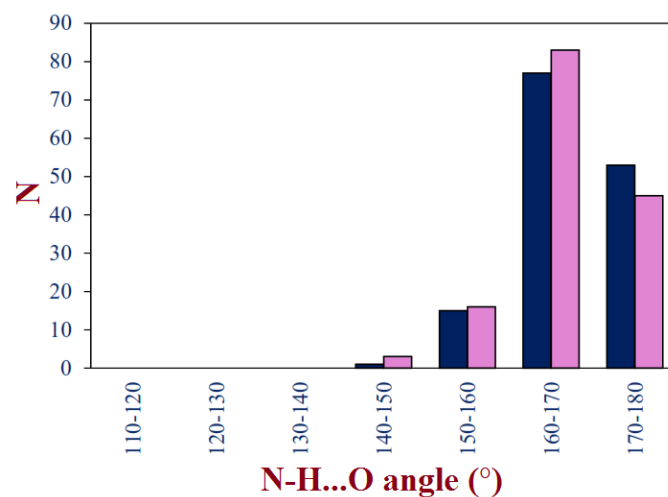efore and after normalization, respectively. In right histogram the hollow columns are related to the angles in $R_2^2(10)$ motifs as black frame (before) and orange frame (after) normalization. The dark blue and pink columns are related to the angles in $R_2^1(6)$ motifs before and after normalization, respectively.

Figure S11. The histogram of N—H…O angles in $R_2^2(8)$ motifs of the $[RC(O)NH]P(O)[NR^1R^2]_2$ structures. The dark blue and pink columns are related to the angles before and after normalization, respectively.
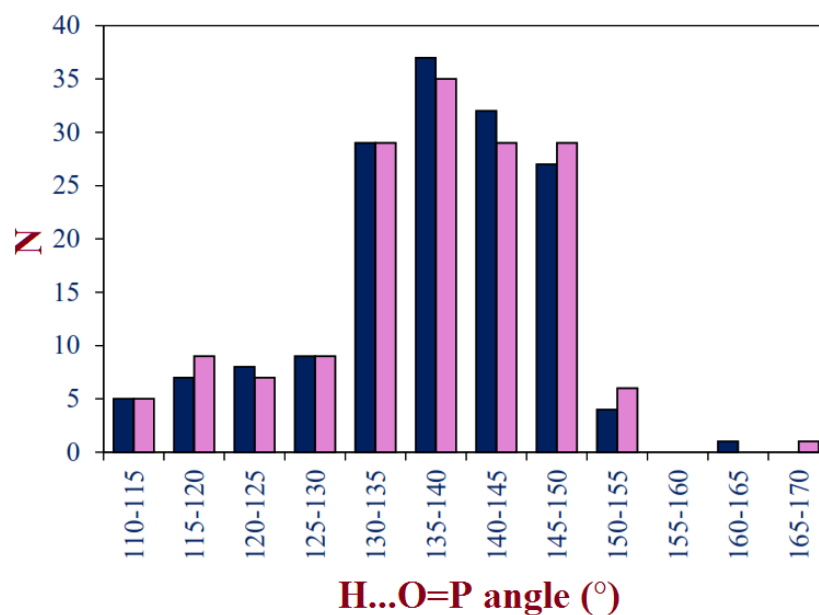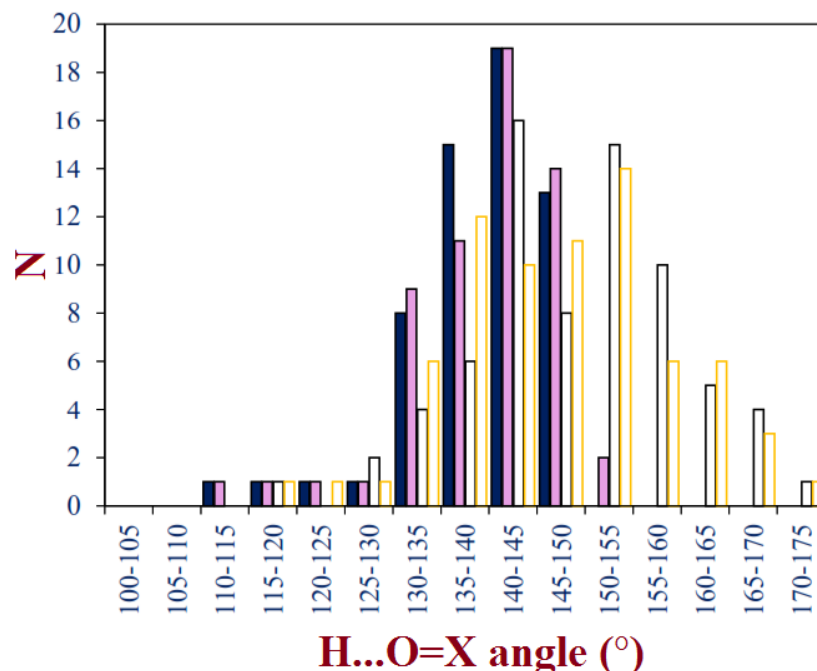

Figure S12. The histogram of H…O=P angles of the $[RC(O)NH]P(O)[NR^1R^2]_2$ structures. The dark blue and pink columns are related to the values before and after normalization, respectively.

Figure S13. The histogram of H…O=X (X = C and P) angles in $R_2^2(8)$ and $R_2^2(12)$ motifs extracted for $[RC(O)NH]P(O)[NHR^1]_2$ structures. The hollow columns are related to the H…O=C angles in $R_2^2(12)$ motifs, as black frame (before) and orange frame (after) normalization. The dark blue and pink columns are related to the H…O=P angles in $R_2^2(8)$ motifs before and after normalization, respectively.
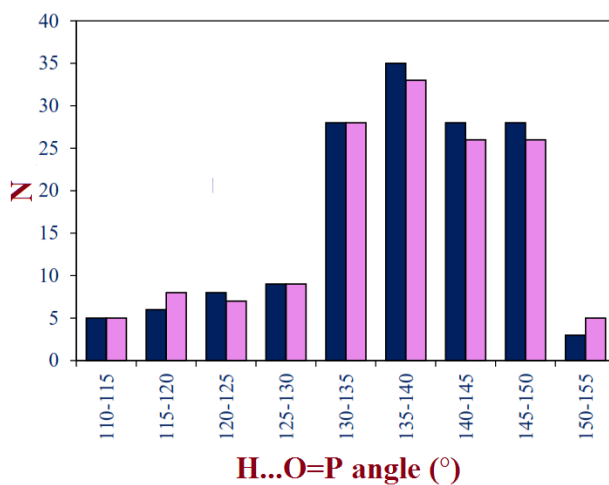

Figure S14. The histogram of H…O=P angles in $R_2^2(8)$ motifs of the $[RC(O)NH]P(O)[NR^1R^2]_2$ structures (the dark blue and pink columns are related to the values before and after normalization, respectively).
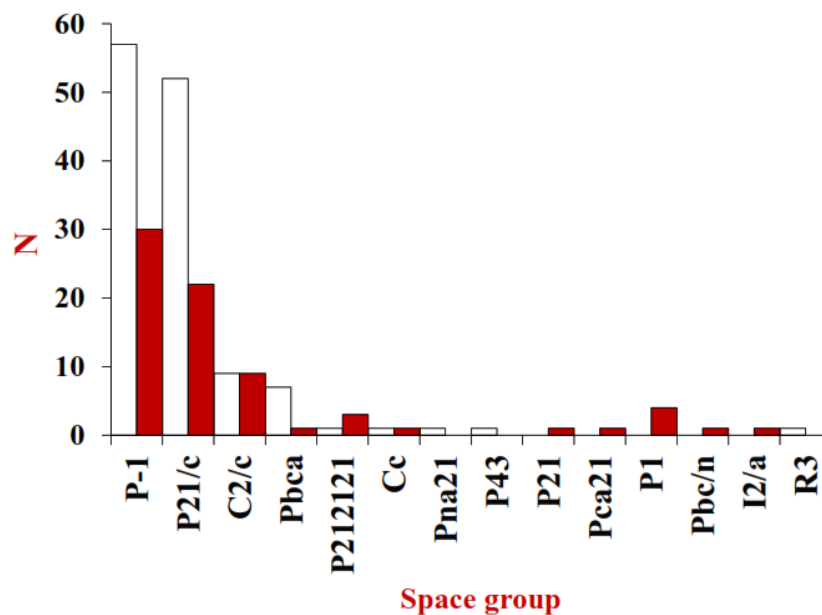
Figure S15. Populations of space groups in the $[R\text{C(O)NH]P(O)[NH}R^1]_2$ (white color) and $[R\text{C(O)NH]P(O)[N}R^1R^2]_2$ (red color) structures.

References

1   Dehghanpour, S., Welter, R., Barry, A. H. & Tabasi, F. (2010). *Spectrochim. Acta*, *Part A***75**, 1236–1243.

2   Gholivand, K., Pourayoubi, M. & Shariatinia, Z. (2007). *Polyhedron*, **26**, 837–844.

3   Drago, R. S. (1992). *Physical Methods for Chemists*, second ed., Saunders College Publishing, Florida, p. 254.